GEOPHYSICAL RESEARCH LETTERS, VOL. 35, L02716, doi:10.1029/2007GL032171, 2008

Deriving historical total solar irradiance from lunar borehole temperatures

Hiroko Miyahara,[1] Guoyong Wen,[2] Robert F. Cahalan,[3] and Atsumu Ohmura[4]

Received 10 October 2007; revised 29 November 2007; accepted 12 December 2007; published 29 January 2008.

[1] We study the feasibility of deriving historical TSI (Total Solar Irradiance) from lunar borehole temperatures. As the Moon lacks Earth's dynamic features, lunar borehole temperatures are primarily driven by solar forcing. Using Apollo observed lunar regolith properties, we computed present-day lunar regolith temperature profiles for lunar tropical, mid-latitude, and polar regions for two scenarios of solar forcing reconstructed by Lean (2000) and Wang et al. (2005). Results show that these scenarios can be distinguished by small but potentially detectable differences in temperature, on the order of 0.01 K and larger depending on latitude, within ~10 m depth of the Moon's surface. Our results provide a physical basis and guidelines for reconstructing historical TSI from data obtainable in future lunar exploration. **Citation:** Miyahara, H., G. Wen, R. F. Cahalan, and A. Ohmura (2008), Deriving historical total solar irradiance from lunar borehole temperatures, *Geophys. Res. Lett.*, *35*, L02716, doi:10.1029/2007GL032171.

1. Introduction

[2] A key prerequisite for understanding human impacts on Earth's changing climate is a reliable estimate of the impacts of solar variations, which in turn requires a definitive reconstruction of long-term variations in the Sun's total solar irradiance (TSI). Variations of TSI, directly measured by radiometers flown onboard several satellites in recent decades, have provided a reliable short-term record of variations since 1978, but this instrumental record has not yet led to a consensus result for solar variations on multi-decadal and longer timescales. Variations of solar activity during recent centuries have been reconstructed from data on sunspots [*Lean*, 2000; *Wang et al.*, 2005] and other indirect proxies such as ^{10}Be in ice cores [*Usoskin et al.*, 2004]. However, these proxy reconstructions have not yet led to any consensus on centennial and longer-term irradiance changes.

[3] New plans to explore the Moon in the near future provide a unique opportunity to resolve this climate conundrum, to complete the lunar heat flow experiment (HFE) first attempted by Apollo 15, to apply it to sharpen limits on the Sun's variations and consequent influence on Earth's climate, and thus the relative importance of the human influences on climate. The time is right to review what was learned from Apollo, to make plans to extend the Apollo experiments, and to perform necessary feasibility studies. We show that measurement of the temperature profile in a lunar borehole enables the reconstruction of TSI back through the Maunder Minimum of solar activity and the Little Ice Age. The potential importance of this for climate change has been emphasized by the National Academy of Sciences [*Committee on the Scientific Context for Exploration of the Moon*, 2007]. The lunar regolith, free of atmosphere, biosphere, hydrosphere and human activities, is directly heated by the variable Sun, so temperature variations at the lunar surface and subsequent heating of the lunar regolith are dominated by variations in the solar input. The observations from HFEs in Apollo 15 and 17 in 1971 and 1972 revealed the lunar regolith's very low thermal diffusivity ($\sim 10^{-8}$ m^2/s) (Table 1). Thus downward propagation of surface temperature variations, induced by solar variations, is confined to the top layer of lunar regolith about 10 m thick, with slower variations appearing in deeper layers (see equation 4 below).

[4] On Earth, long-term surface temperature variations are forced by changes in atmospheric and oceanic composition and dynamics, and not only solar variations. As on the Moon, surface land temperature variations propagate downward and are recorded in terrestrial borehole temperature profiles. The terrestrial borehole project was successfully conducted with several boreholes of ~500 m depth [*Huang et al.*, 2000] to derive surface temperature changes for the last 500 years. Reconstructed surface temperature variations from these boreholes show gradual warming since the 16th century, with more rapid warming during the second half of the 20th century, in agreement with the instrumental record, and with dendroclimatology based on tree-ring width patterns [*Mann et al.*, 1999].

[5] This paper reports the feasibility of reconstructing TSI from the lunar regolith using a heat flow model with observed thermal properties from Apollo HFEs for two TSI scenarios [*Lean*, 2000; *Wang et al.*, 2005]. We first describe the exploration plan for HFEs on the moon in section 2, then briefly review the HFEs during the Apollo mission in section 3. The heat flow model is described in section 4, followed by the results in section 5. The results are summarized and discussed in the final section 6.

2. Exploration Plans

[6] Let us summarize requirements for a successful experiment. First, we must determine the optimal depth of

[1] Department of Earth and Planetary Science, University of Tokyo, Tokyo, Japan.
[2] Goddard Earth Sciences and Technology Center, University of Maryland Baltimore County, Baltimore, Maryland, USA.
[3] Laboratory for Atmospheres, NASA Goddard Space Flight Center, Greenbelt, Maryland, USA.
[4] Institute for Atmospheric and Climate Sciences, ETH Zurich, Zurich, Switzerland.

0094-8276/08/2007GL032171$05.00

Table 1. Input Parameters for the Heat Flow Model From *Keihm*, [1984][a]

Parameters		Formula
$\rho(z)$	*density* (kg/m^3)	$\rho(z) = 1250 \quad (z \le 0.02m)$ $= 1900 - 650\exp\left[\frac{0.02-z}{0.04}\right] (z > 0.02m)$
$k(z, T)$	*thermal conductivity* ($W/m \cdot K$)	$k(z,T) = k_1(z) + k_2 \cdot T^3$ $k_1(z) = k_s \quad (z \le 0.02m)$ $= k_d - (k_d - k_s) \cdot \exp\left(\frac{0.02-z}{0.04}\right) \quad (z > 0.02m)$ $k_s = 6 \times 10^{-4}\ W/m \cdot K$ $k_d = 8.25 \times 10^{-3}\ W/m \cdot K$ $k_2 = 3.78 \times 10^{-11}\ W/m \cdot K^4$
$C(T)$	*specific heat* ($J/kg \cdot K$)	$C(T) = 670 + 10^3(\frac{T-250}{530.6}) - 10^3(\frac{T-250}{498.7})^2$
$\varepsilon(T_s)$	*emissivity*	$\varepsilon(T_s) = 0.9696 + 0.9664 \times 10^{-4}\ T_s - 0.31674 \times 10^{-6}\ T_s^2 - 0.50691 \times 10^{-9}\ T_s^3$ where T_s is the surface temperature
$\alpha(\theta_0)$	*albedo*	$\alpha(\theta_0) = 0.12 + 0.03(\theta_0/45)^3 + 0.14(\theta_0/90)^8$ where θ_0 (solar zenith angle in degree) is computed from JPL ephemerides
H	*internal heat flux* (W/m^2)	$H = 0.018\ W/m^2$
$d(t)$	*distance* (AU)	Moon-Sun distance in astronomical unit (AU) computed from JPL ephemerides
$TSI(t)$	*Total Solar Irradiance* (W/m^2)	Total solar irradiance at 1 AU

[a]Note that thermal diffusivity is given by K = k/(ρC) and for typical range of surface temperature is $2-7 \times 10^{-9}$ m^2/s, with higher values at higher temperatures. Moon–Sun distance and total solar irradiance are also defined.

lunar regolith to measure temperature anomalies induced by solar variability. We show in section 5 below that a lunar borehole temperature profile extending to 10 m depth, and of sufficient precision to resolve a temperature anomaly of about 0.01 K, is required. We demonstrate that the signatures of multi-centennial TSI variations are preserved in the upper layer ~10 m of lunar regolith, and that the range of temperature anomalies expected is about 0.01~0.015 K.

[7] Second, the Moon is not uniformly covered with regolith so drilling sites need to be carefully selected since. Lunar regolith, the top sector of accumulated pulverized rock on top of the bedrock of the moon, grows as a result of micro-meteorite impacts, and extends to a depth of a few meters to 10s of meters [*Muehlberger et al.*, 1972]. Seismographic data indicates that the regolith at the site of Apollo 16 is 12.2 m [*Horvath et al.*, 1980; Y. Nakamura, personal communication, 2007]. High altitude plateaus of old geological sites hold thick layers of regolith. The regolith in more recently created craters is only a few meters thick. Deeper regolith enables longer reconstruction of TSI. Thus highlands without any physical disturbance in historical times are prime candidates for heat flux experimental sites. Temperature anomalies induced by TSI variations are largest near the equator, and potentially detectable near the lunar poles. Measurements at either low or high latitudes are theoretically sufficient for reconstructing historical TSI. Further, a polar site may have the advantage of providing continuous solar power, while an equatorial experiment would need to survive the frigid lunar darkness.

[8] Third, since the temperature anomaly driven by long term solar forcing is small, any thermal or physical disturbance could contaminate the recorded history of TSI in the regolith, and may invalidate a purely solar interpretation of the observations. Thus the experiments should be conducted under well-managed conditions that assure minimum thermal disturbance. An operations plan will be needed that assures minimum thermal disturbance. More than one borehole measurement is preferred to check the consistency.

[9] The experiment we propose is an extension to the Apollo HFEs, with enhanced precision, and the emphasis shifted from the temperature profile itself to nonlinear deviations due to historical solar irradiance variations. As with the HFEs, this experiment requires measurement of regolith thermal and radiative properties. Borehole samples are also of interest for other lunar exploration research, including the study of the structure and composition of the Moon, and the search for lunar resources. A base on the Moon for systematic measurements at several sites would enable a series of robotic experiments. Borehole temperature profiles from robotic missions could provide initial precise examinations of the heat flow of the Moon, and could then be extended to other sites with support from a permanent Moon base.

3. Review of Apollo 15 and 17 Heat Flow Experiments (HFEs)

[10] During the pioneering Apollo Moon missions, spacecraft landed on the Moon six times, and conducted several experiments including the HFEs. The HFEs were designed to estimate the rate of internal heat production by long-lived radioisotopes by measuring the properties of heat propagation in lunar subsurface layers. Temperatures were measured using two temperature-sensing probes with eight thermocouples embedded in the lunar subsurface spaced ~10 m apart. The thermocouples were attached to the probes so that the temperatures and the thermal diffusivity could be measured at different depths. Subsurface temperature variations were obtained with accuracy ±0.05 K for more than 3.5 years by Apollo-15 and 17 [*Langseth et al.*, 1972, 1973].

[11] Surface temperatures were observed from the HFEs during Apollo-15. Surface temperature rises quickly after sunrise reaching ~370 K at the daytime maximum. Surface temperature drops rather rapidly during sunset. The nighttime temperature decrease gradually reaches a minimum ~100 K (see example in section 4). The large diurnal variation of surface temperature, from ~100 K during the lunar nighttime minimum to ~370 K at the lunar daytime maximum, is a result of the combination of low thermal diffusivity and the absence of atmosphere. Thermal diffusivity of lunar regolith is about $2\sim7 \times 10^{-9}$ m^2/s [*Keihm*,

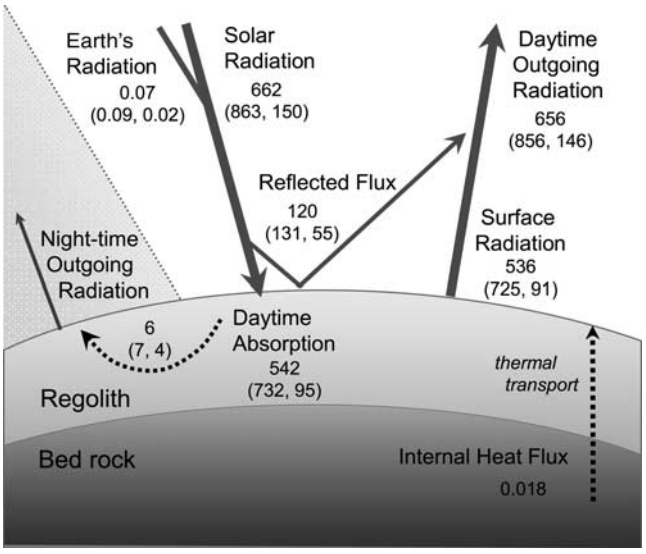

Figure 1. Energy balance of lunar system with unit of W/m^2 for mid-latitude. Energy budgets for the equator and the polar sites, respectively, are presented in parentheses.

1984] (see Table 1), about two orders of magnitude smaller than that of Earth's crust [*Seipold and Gutzeit*, 1982]. The thermal and radiative properties of the lunar regolith compiled by *Keihm* [1984] are presented in Table 1, and applied in the next sections.

4. Heat Flow Model

[12] Profiles of the lunar regolith temperature $T(z, t)$ as a function of depth z and time t are governed by the standard heat diffusion equation, given by

$$\rho(z)C(T)\frac{\partial T(z,t)}{\partial t} = \frac{\partial}{\partial z}\left(k(z,T)\frac{\partial T(z,t)}{\partial z}\right) \quad (1)$$

with boundary conditions

$$k(z,T)\frac{\partial T(z,t)}{\partial z}\bigg|_{z=0} = \varepsilon(T)\sigma T(0,t)^4 - (1-\alpha(\theta_0(t)))\cos(\theta_0(t))TSI(t)/d(t)^2 \quad (2)$$

$$k(z,T)\frac{\partial T(z,t)}{\partial z}\bigg|_{z=z_b} = H \quad (3)$$

The regolith thermal and radiative properties needed in equations (1)–(3) are provided in Table 1. Note that thermal conductivity and specific heat have strong dependences on temperature. These properties are derived from Apollo data. Here we use them for planning, but expect that they will be measured in detail for each new site. Since TSI is adjusted to d = 1AU, we use the JPL Planetary and Lunar Ephemerides [*Standish*, 1998] to compute Moon-Sun distance $d(t)$ and the solar zenith angle $\theta_0(t)$. The net radiative flux (i.e., the sum of emitted thermal radiation and the absorption of solar radiation, the first and the second terms on the right hand side of equation (2) respectively) determines the heat flow at the upper boundary. Equation (3) describes the net heat flow from below at the lower boundary of the computational domain, $z = z_b$.

[13] Figure 1 shows schematically the relative magnitude of the three individual energy budget terms in equation (2), averaged separately over day and night, at latitude 0°, 40° S, 80° S, and for TSI 1361 W/m^2 [*Kopp et al.*, 2005]. During daytime, the Sun provides an average input of about 662 W/m^2 at the lunar surface at mid-latitudes, with 120 W/m^2 reflected back to space, leaving 542 W/m^2 to be absorbed by the regolith layer. The absorbed solar radiation is not balanced by the emitted thermal radiation of about 536 W/m^2. The average net energy flux is about 6 W/m^2, and is transported downward and stored as heat in the top layer (~0.5 m thick) of the regolith. During the lunar night, this heat stored during the lunar day is transported to the surface and emitted to space. Radiation from the Earth is about 1~2 orders of magnitude smaller than the heat storage and thus near the surface at the Apollo sites, it can safely be ignored. (However, terrestrial radiation is ~1 order of magnitude larger than the internal heat flux H = 0.018 W/m^2 and so becomes important in permanently shaded regions.) The energy budgets may not be precise; however, the sketch in Figure 1 quantifies the relative importance of each individual term in determining the surface temperature of the Moon.

[14] We check model performance by comparing modeled temperatures to observations at the Apollo-15 site. As seen in Figures 2a and 2b, numerical results adequately reproduce the observed surface temperatures except near sunrise and sunset. Differences between modeled and observed surface temperature near sunrise and sunset are likely due to local surface topographic variations [e.g, *Langseth et al.*, 1972] not accounted for in our 1D model. During the Apollo HFEs total solar eclipses occurred several times at the Apollo 15 site, resulting in abrupt decreases in the surface temperature at solar noon. As our interest is in climatic changes, these short time disturbances are ignored in the modeling study.

[15] In order to fully understand the relationship between the historical TSI variations and consequent impacts on the present-day lunar borehole temperatures we need to solve the governing equation (1). The input historical variation of TSI is not well known. This can be seen in two scenarios of reconstructed TSI (Figure 3a). The two scenarios agree well in the recent solar 11-year cycles, but differ by about 2 W/m^2 during Maunder Minimum about 330 years ago. Using the two scenarios as inputs in the numerical computations, we consider whether the temperature responses are distinguishable. Some argue for a smaller solar variation [e.g., *Foukal et al.*, 2004], which might produce an undetectable lunar signal. Our purpose here, however, is not to decide which scenario is correct, but to show that particular solar scenarios can potentially be excluded by the borehole measurement, which would narrow the range of possibilities.

5. Model Results

[16] As a first step in understanding the behavior of heat penetration in the lunar regolith, we examine the e-folding depth for ideal periodic temperature variations at the surface. For a homogeneous medium of diffusivity K, with a

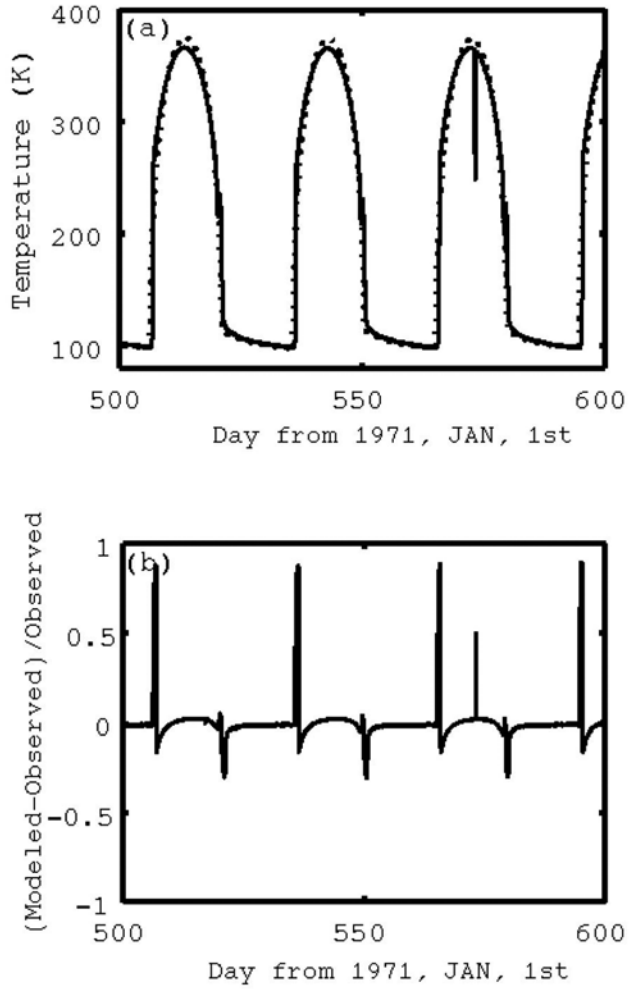

Figure 2. (a) Lunar surface temperatures obtained by HFE of Apollo 15 (solid line) and the modeled surface temperatures obtained for the same site (dotted line). (b) Relative difference between modeled and observed surface temperatures.

sinusoidal surface temperature variation, the e-folding penetration depth is given by:

$$z_e = \sqrt{\frac{KP}{\pi}} \tag{4}$$

where P is the period of the variation. This equation follows from a simple scaling argument, and the proportionality constant may be determined from equation (1).

[17] Setting P = 1 year $\approx \pi \times 10^7$ s, we find that monthly and annual periodic variations of temperature at the surface are strongly attenuated within the top 0.3 m of the regolith. Variations in TSI related to 11-year solar activity are primarily confined to the first couple of meters of regolith. For a timescale of about 400 years (or $P \sim 800$ years) for the Maunder Minimum, the penetration depth is about 8 meters. Therefore, a typical 10 m deep borehole is required in reconstructing TSI back to the Maunder Minimum. Also, exponential attenuation of the periodic variations indicates that we will need high-precision measurements in reconstructing TSI from lunar regolith temperatures. The temporal resolution (Δt) of periodic temperature variations at the surface is half of the period. Thus equation 4 also determines the temporal resolution of a surface variation as it diffuses downward to z_e: $\Delta t = P/2 = 0.5\ \pi z_e^2/K$.

[18] The penetration depth provides a rough estimate of regolith depth required to resolve TSI variations on timescales of interest. In reality thermal properties of the regolith depend on temperature (see Table 1 for the Apollo parameters used here, which new experiments will need to reexamine). The surface temperature is not a simple sinusoidal, and historical solar forcing plays an important role in the lunar regolith temperature profile. A detailed analysis is needed to estimate the vertical structure of temperature anomalies as a result of long-term solar forcing by solving equations (1)–(3). Two present-day temperature profiles $T_1(z)$ and $T_2(z)$ in year 2000 AD are computed from the fully coupled radiation, heat conduction, and heat diffusion system (i.e., equations (1)–(3)) using the two TSI scenarios of *Lean* [2000] and of *Wang et al.* [2005] for 1610–2000 AD, respectively. Using the difference of the two temperature

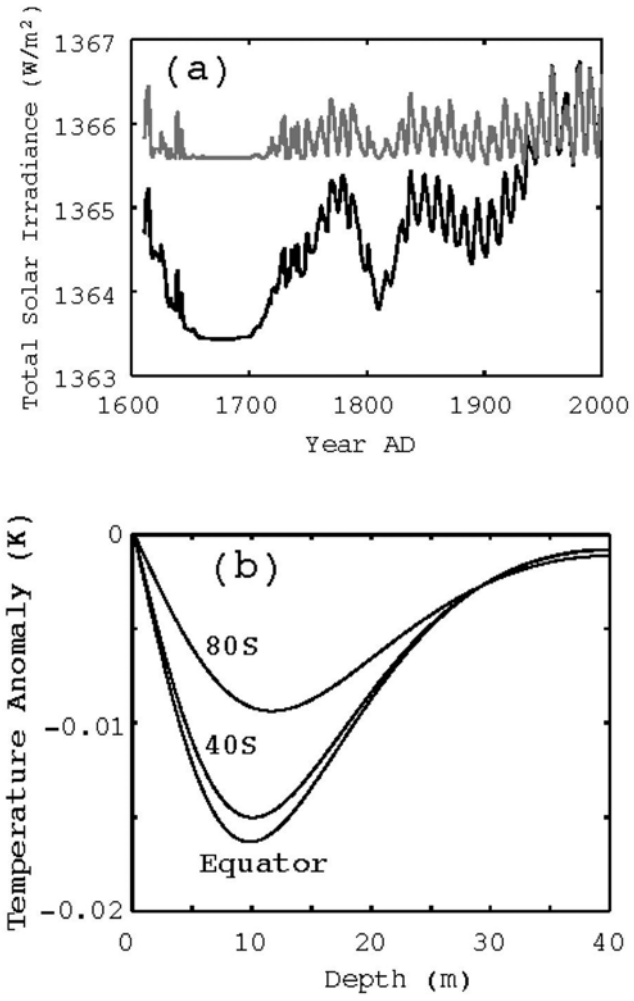

Figure 3. (a) TSI scenarios by *Lean* [2000] (black line) and *Wang et al.* [2005] (gray line) define the solar input of to the heat flow computations. (b) Temperature anomalies as response to two scenarios of reconstructed TSI in Figure 3a at the equator, mid-latitude (40°S), and near the south pole (80°S).

profiles, we examine the possible temperature anomalies (*i.e.*, $\Delta T(z) = T_1(z) - T_2(z)$) caused by different solar forcing given by these two scenarios. Because the high-frequency signal is attenuated at the very top layer of the regolith (see equation (4)), one expects to see smooth temperature anomalies induced by centennial time scale TSI variations.

[19] Figure 3b shows the temperature anomalies expected for an equatorial, mid-latitude and polar site. Since the timescales for both TSI models are about the same as reductions in TSI during the Maunder Minimum, a larger reduction of TSI in the case of *Lean* [2000] leads to a negative anomaly compared to the scenario of *Wang et al.* [2005]. The magnitude of temperature anomaly increases as a function of depth, reaching a maximum of 0.016 K, 0.015 K, and 0.009 K for the equatorial, mid-latitude, and polar sites, respectively, at a depth of about 10 m, and decreases gradually as it gets deeper. The magnitude of the peak of the temperature anomaly depends on the latitude. However the depth where the peak occurs is independent of latitude. This is consistent with the penetration depth defined in equation (4).

6. Summary and Discussion

[20] We have examined the feasibility of using lunar temperature profiles to reconstruct TSI back to the Maunder Minimum. We determined the lunar borehole temperature response to two reconstructed TSI time series. We found that (1) the signals of variations of TSI in centennial timescales are recorded as temperature anomalies confined in an optimal depth about 10 m thick in lunar regolith; (2) the magnitude of optimal temperature anomaly ranges from $\sim$0.01 K near the lunar poles to $\sim$0.017 K at the equator. The optimal depth of 10 m is consistent with the simple penetration depth derived from dimensional analysis.

[21] Our results are based on regolith thermal parameters determined by the Apollo experiments. Re-measurement of the regolith parameters will be an important early science goal during our return to the Moon. With similar TSI in the few recent solar cycles, the two historical TSI scenarios diverge about 70 years before the present, with the largest difference about 2 W/m^2 during the Maunder Minimum around 330 years ago. These two scenarios represent the current understanding of variations of TSI on the centennial timescale. To distinguish the two TSI scenarios requires a temperature measurement precision that can resolve temperature differences of 0.01 K in a lunar borehole about 10 m deep.

[22] In order to achieve accurate reconstruction of TSI from lunar borehole temperatures, a location near the equator is most desirable, although the signal of TSI variations in lunar borehole temperatures is smaller but potentially detectable near the lunar poles. Since the heat flow depends on thermal conductivity, density and specific heat, the experiment requires measurements of these parameters with high spatial resolution in addition to the temperatures. Those parameters can be obtained from observations during future exploration.

[23] This research provides the fundamental physical basis and guidelines for reconstructing TSI back to the time period of the Maunder Minimum and Little Ice Age from lunar borehole temperatures. The results reported here are based on 1D computations and Apollo HFE derived thermal properties. In reality, the terrain of the lunar surface, bedrock with higher thermal conductivity at some depth and other possible heat sources and their variations, may affect borehole temperature profiles. In future research, we plan to extend the current 1D model to a 3D model to account for the observed topography of specific proposed experimental sites. We will further study the impact of the bedrock and other potential heat sources on borehole temperature profiles, and on reconstructions of historical values of TSI.

[24] **Acknowledgments.** We thank Judith Lean for providing the TSI forcing scenarios. We deeply appreciate Myles Standish for his support concerning the JPL ephemerides. We also thank Shaopeng Huang, Stephen Keihm, George Lawrence, Norman Loeb, Paul Lowman Jr., and Yasuyuki Saito for their suggestive comments and fruitful discussion and Ken Hills for providing Apollo HFE data sets. We thank Y. Nakamura for discussions on lunar seismography and regolith depth. We also thank David Sibeck for his support in arranging this project. G. W. and R. C. thank NASA's LWS TR&T program. H. M.'s work is supported by the Grant-in-Aid for JSPS Research Fellows. H. M. greatly appreciates the Climate and Radiation Branch of NASA/Goddard Space Flight Center for hosting her visit.

References

Committee on the Scientific Context for Exploration of the Moon (2007), *The Scientific Context for Exploration of the Moon,* 120 pp., Natl. Acad. Press, Washington, D. C.

Foukal, P., G. North, and T. Wigley (2004), A stellar view on solar variations and climate, *Science*, *306*, 68–69.

Huang, S., H. N. Pollack, and P. Y. Shen (2000), Temperature trends over the past five centuries reconstructed from borehole temperatures, *Nature*, *403*, 756–758.

Horvath, P., G. V. Latham, Y. Nakamura, and H. J. Dorman (1980), Lunar near-surface shear wave velocities at the Apollo landing sites as inferred from spectral amplitude ratios, *J. Geophys. Res.*, *85*, 6572–6578.

Keihm, S. J. (1984), Interpretation of the lunar microwave brightness temperature spectrum: Feasibility of orbital heat flow mapping, *Icarus*, *60*, 568–589.

Kopp, G., G. Lawrence, and G. Rottman (2005), The Total Irradiance Monitor (TIM): Science results, *Sol. Phys.*, *203*, 129–139.

Langseth, M. G., S. P. Clark, J. L. Chute, S. J. Keihm, and A. E. Wechsler (1972), Heat flow experiment, in *Apollo 15 Preliminary Science Report*, *Rep. NASA SP-289*, pp. 11-1–11-23, NASA, Washington, D. C.

Langseth, M. G., S. J. Keihm, and J. L. Chute (1973), Heat flow experiment, in *Apollo 17 Preliminary Science Report*, *Rep. NASA SP-330*, pp. 9-1–9-24, NASA, Washington, D. C.

Lean, J. (2000), Evolution of the Sun's spectral irradiance since the Maunder Minimum, *Geophys. Res. Lett.*, *27*, 2425–2428.

Mann, M. E., R. S. Bradley, and M. K. Hughes (1999), Northern hemisphere temperatures during the past millennium: Inferences, uncertainties, and limitations, *Geophys. Res. Lett.*, *26*, 759–762.

Muehlberger, W .R., et al, (1972), Preliminary geologic investigation of Apollo 16 landing site, in *Apollo 16 Preliminary Science Report*, *Rep. NASA SP-315*, pp. 6-1–6-81, NASA, Washington, D. C.

Seipold, U., and W. Gutzeit (1982), The distribution of thermal diffusivity in Earth's crust, *Phys. Earth Planet. Int.*, *29*, 69–72.

Standish, E. M. (1998), JPL planetary and lunar ephemerides, *JPL IOM 312,* Jet Propul. Lab., Pasadena, Calif.

Usoskin, I. G., K. Mursula, S. Solanki, M. Schüssler, and K. Alanko (2004), Reconstruction of solar activity for the last millennium using ^{10}Be, *Astron. Astrophys.*, *413*, 745–751.

Wang, Y. M., J. L. Lean, and N. R. Sheeley (2005), Modeling the Sun's magnetic field and irradiance since 1713, *Astrophys. J.*, *625*, 522–538.

R. F. Cahalan, Laboratory for Atmospheres, NASA Goddard Space Flight Center, Mail Code 613.2, Greenbelt, MD 20771, USA.

H. Miyahara, Department of Earth and Planetary Science, University of Tokyo, 7-3-1 Hongo, Bunkyo-ku, Tokyo 113-0033, Japan.

A. Ohmura, Institute for Atmospheric and Climate Sciences, ETH Zurich, Winterhurerstrasse 190, CH-8092 Zurich, Switzerland.

G. Wen, Goddard Earth Sciences and Technology Center, University of Maryland Baltimore County, 5523 Research Park Drive, Suite 320, Baltimore, MD 21228, USA. (wen@climate.gsfc.nasa.gov)